SURFACE IGNITION IN A STEADY-FLOW APPARATUS

Edmund W. Sellman
and
John E. Snyder

SURFACE IGNITION IN A STEADY-FLOW APPARATUS

by

Edmund W. Sellman, Lt., U.S. Navy

S.B.A.E., Massachusetts Institute of Technology
(1946)

S.B.A.E., U.S. Naval Postgraduate School
(1955)

and

John E. Snyder, Lt., U.S. Navy

S.B., U.S. Naval Academy
(1946)

S.B.A.E., U.S. Naval Postgraduate School
(1955)

SUBMITTED IN PARTIAL FULFILLMENT
OF THE REQUIREMENTS FOR THE
DEGREE OF MASTER OF SCIENCE
AT THE
MASSACHUSETTS INSTITUTE OF TECHNOLOGY
June 1956

Signature of Authors .....
Department of Aeronautical Engineering, May 21, 1956

.....
Department of Aeronautical Engineering, May 21, 1956

Certified by .....
Thesis Supervisor

Accepted by .....
Chairman, Departmental Committee on Graduate Students

SURFACE IGNITION IN A STEADY-FLOW APPARATUS

by

Edmund W. Sellman

and

John E. Snyder

(Submitted to the Department of Aeronautical Engineering on May 21, 1956 in partial fulfillment of the requirements for the degree of Master of Science in Aeronautical Engineering.)

ABSTRACT

A study is made of the surface temperature required for ignition of a pre-mixed stoichiometric ethanol-air mixture in steady flow. The surface temperature of a Nichrome V tube two inches long and one-half inch in diameter is increased by means of induction heating until the mixture flowing at a controlled velocity, density, and inlet temperature is ignited. Ignition is detected visually. A range of flow velocities from 20 to 70 ft./sec at free stream densities of 0.0575, 0.0484, and 0.0393 lbs./cu.ft. was investigated. The inlet mixture temperature was maintained constant at 634°R.

Examination of the resulting temperature-velocity curves reveals that the surface temperature required for ignition increases with an increase in velocity, forming a concave-downward curve. All the data were reduced to a single curve by plotting the surface temperature versus the density-to-velocity ratio. Very good correlation was obtained on this basis except that there was a tendency for the values taken at higher density to fall below the mean curve through the data. The data were reproducible to $\pm$10°F.

Cambridge, Massachusetts
May 21, 1956

Professor Leicester F. Hamilton
Secretary of the Faculty
Massachusetts Institute of Technology
Cambridge, Massachusetts

Dear Sir:

A thesis entitled "Surface Ignition in a Steady-Flow Apparatus" is herewith submitted in partial fulfillment of the requirements for the degree of Master of Science in Aeronautical Engineering.

Respectfully,

Edmund W. Sellman

John E. Snyder

ACKNOWLEDGMENT

The authors are greatly indebted to Professor T. Y. Toong for his patient guidance throughout this investigation. Professor E. S. Taylor, and Mr. J. C. Livengood have offered many helpful suggestions. Mr. G. F. Harper extended his time and experience freely to aid in setting up and calibrating the apparatus. The entire personnel of the Sloan Automotive Laboratory have been most helpful and cooperative. Mr. Joseph Calogerro offered much valuable assistance in coping with the inevitable mechanical difficulties.

TABLE OF CONTENTS

LIST OF ILLUSTRATIONS

NOMENCLATURE

A	Cross-sectional area of the test section (ft^2)
A'	Internal surface area of the test section (ft^2)
a	Rate of consumption of combustible per unit volume
E	Activation energy
c	Partial density of combustible component in mixture
K	Specific reaction rate
k	Coefficient of thermal conductivity (watts/sec cm°C)
p_o	Pressure of mixture at nozzle (In.Hg.)
p_1	Pressure before ASME orifice (In.Hg.)
Δp	Differential pressure across orifice (In. H_2O)
q	Heat transferred (watts)
R	Gas constant of mixture (51.4 ft.lb/lb°F)
T_o	Inlet-mixture temperature (°R)
T_1	Air temperature before orifice (°R)
T_n	Nozzle wall temperature (°F)
T_a	Apparent surface temperature (°F)
T_w	True surface temperature (°R)
V	Flow velocity in the test section (ft/sec)
w	Total mass flow (lbs/sec)
w_a	Air flow (lbs/sec)
w_f	Fuel flow (lbs/sec)
ε	Emissivity
ρ_o	Inlet mixture density (lbs/ft^3)

1 Introduction

The ignition of a homogeneous fuel-air mixture by means of a hot surface in a steady-flow device is investigated experimentally. Much of the experimental ignition research which has been done involves devices that protrude into the stream, thereby complicating the flow pattern so that theoretical analysis becomes impractical. An investigation has been started at the Massachusetts Institute of Technology with a simplified flow pattern in order that theory and experiment may be compared directly. An approach to the problem for which theoretical solutions can be obtained assumes a homogeneous combustible mixture in laminar flow over a uniformly heated flat plate. The theoretical conditions are nearly met by the experimental equipment. This consists of a steady-flow apparatus in which a pre-mixed fuel-air mixture flows past a heated surface which forms part of the containing pipe, so that no obstruction to the flow is present. The surface temperature required to initiate combustion is determined by establishing the flow at given conditions and then increasing the surface temperature until ignition occurs.

A survey of the literature failed to reveal any research with this type of apparatus other than that performed at the Massachusetts Institute of Technology. Experimental work was performed by Davis (Ref. 1) and by Barkah (Ref. 2). The former designed the apparatus which provided for heating a two inch long 60° sector of a one-half inch pipe with an oxy-acetylene torch. Ignition was detected by a spark plug ionization gap. The surface temperature of the heated section was measured with thermocouples. Davis' results showed that the basic apparatus was satisfactory for this type of investigation.

Barkah modified Davis' equipment by installing three quartz windows opposite the heated sector. This allowed an optical pyrometer to be used to measure the test section temperature. Barkah investigated the effects of the temperature of the mixture at the inlet to the test section, the inlet-density, and the flow velocity on the temperature required for ignition. He found that the surface temperature required to ignite the mixture is inversely proportional

to the inlet-mixture temperature if all other conditions remain constant. His results showed that the surface temperature required for ignition increased with an increase of velocity, forming a concave-downward curve on a plot of surface temperature versus velocity. Limited data also indicated that the effect of lowering the density was equivalent to raising the velocity.

The apparatus used by Barkah and Davis has been modified to provide uniform circumferential heating by means of high-frequency induction heating. This has resulted in more precise temperature control, and a reduction of leakage problems previously encountered. Temperature-velocity relations for ignition at various densities have been investigated and compared with theory.

The theory has been proposed by Professor T. Y. Toong of the Massachusetts Institute of Technology in which the development of combustion is studied by use of boundary-layer theory (Ref. 3). This theory assumes laminar flow over an isothermal flat plate of a perfect gas with constant properties except that the viscosity varies directly with the absolute temperature. It is assumed that the chemical reaction which proceeds in the boundary layer is one of the second order of the Arrhenius type, such that the rate of consumption of combustible component per unit volume, a, equals $K\rho^2 c^2 \exp(-E/RT)$. The second-order theory indicates that if free-stream velocity varies directly with the free-stream density, incipient ignition occurs at the same value of surface temperature for the same free-stream temperature. The applicability of this theory to the ignition of a stoichiometric ethyl alcohol-air mixture is investigated in this report.

2 Apparatus

The flow diagram, Fig. 1, schematically illustrates the apparatus used in this investigation. The basic design of J. W. Davis has been utilized with modifications to the test section. Detailed descriptions and drawings of the inlet, exhaust, and fuel systems may be found in Ref. 1.

2.1 General Description

Air, supplied either from the atmosphere by means of a vacuum pump or from a compressor, is metered by a standard ASME orifice prior to entering a mixing tank. Fuel (ethyl alcohol) is sprayed into the air stream immediately upstream of the mixing tank. The tank is surrounded by a steam jacket to heat the mixture to the proper temperature and to insure complete fuel vaporization. The heated mixture flows through a straightening section to a converging nozzle before passing through the test section (Fig. 2). The test section is heated by an induction coil. The temperature of the mixture is measured by shielded thermocouples placed in the stream at the exit of the mixing tank and immediately upstream from the nozzle. The nozzle wall temperature is also measured by a thermocouple. An optical pyrometer is used to measure the test section temperature. Downstream from the test section is an exhaust tank fitted with spark plug ignition and spray nozzles to burn and cool the mixture before it flows out through the exhaust system. It was found that burning the mixture in the tank and using the spray nozzles caused pulsations in the flow; therefore, they were not used. As a safety measure, the exhaust mixture was diluted with air downstream from the exhaust tank.

2.2 Test Section

The test section consists of a Nichrome V tube two inches long with a wall thickness of 0.015 inches (Fig. 3). (Nichrome V is the trade name of an alloy containing 80 per cent nickel and 20 per cent chromium. It is produced by the Driver-Harris Company and is extensively used for high temperature electrical applications.) Flanges at each end of the test section reduced warping and helped prevent leakage. Lava A ceramic insulators (Fig. 3) reduced axial conduction

to a low level, making it possible to obtain an essentially constant temperature over 72 per cent of the test section. These insulators also positioned the induction heating coil. The test section, gaskets, and insulators were aligned with the nozzle by inserting a rod 0.499 inches in diameter down through the assembly. After the test section was centered, the rod was withdrawn and the downstream tubing secured in position.

2.3 Induction Heating Coil

An induction coil was used to obtain circumferentially symmetric heating over the length of the test section. The power for the coil was provided by a Westinghouse one-kilowatt radio-frequency generator operating at 300 kilocycles. The operation of this machine is described in Appendix III. The water-cooled coil consisted of 16 turns of 1/8 inch copper tubing with variable spacing. Since the coil did not match the generator, 0.06 microfarad capacitance was added in parallel to the work coil to improve the power factor. This arrangement allowed temperatures up to 2200°F to be obtained with flow rates approaching 100 feet per second. The coil spacing was adjusted to obtain the optimum temperature distribution. This adjustment could be made with the equipment assembled. Appendix II describes the method used to obtain the temperature distribution. The temperature distribution with an evenly spaced coil and the final temperature distribution employed in the investigation are shown in Fig. 4.

2.4 Minor Design Changes

A 15 mm. vicor glass tube 24 inches long was inserted immediately downstream from the test section to permit the operator to detect ignition visually and to examine the flame (Fig. 2). The ends of the test section and the sight glass were effectively sealed by using rubberized asbestos gaskets at each joint and putting axial compression on the system by means of springs. These springs also allowed for expansion and contraction of the system. The pressure drop in the system with time is shown in Fig. 5.

The nozzle cooling system as described in Ref. 1 was altered to provide circumferential cooling. The existing cooling sector was plugged and a 1/8 inch by 1/8 inch groove was cut around the nozzle at the throat. The rate of coolant flow in this passage was regulated to maintain a nozzle wall temperature between 100°F and 120°F.

A steam heating coil incorporated around the pipe upstream from the nozzle permitted more accurate control of the inlet temperature and materially shortened the warm-up period.

3 Test Procedure

The principal variables involved in this investigation are flow velocity, mixture density, inlet mixture temperature, fuel-air ratio, type of fuel, and the surface temperature. The test procedure was designed to determine the effect of velocity on surface temperature required for ignition at various densities. Surface temperature was maintained as the dependent variable at all times. Fuel, fuel-air ratio, and inlet-mixture temperature were maintained constant throughout the tests. The fuel used was ethanol, the fuel-air ratio was stoichiometric (0.111) and the inlet mixture temperature was 634°R. A value of density was established and a series of tests at various velocities conducted. The procedure was then repeated at a different density.

After choosing a value of density and velocity for a particular test, steady state conditions were achieved and maintained up to the point where ignition occurred. The procedure outlined below was followed.

1. Heat the test section to approximately 20° below the expected temperature for ignition.
2. Check all observed pressures and temperatures for correct readings.
3. Increase the power output of the induction heater enough to obtain a 3-6°F increase in the test section temperature.
4. After equilibrium has been reached, balance and read the optical pyrometer.
5. Repeat steps 3 and 4 until the first flame is observed visually. (Ignition can also be detected by a sharp fluctuation on the manometer board and also by a rapid increase in the test section temperature.)
6. Record all temperatures, manometer readings, and the rotometer reading at the point of ignition.
7. Repeat the run if there is any doubt as to the validity of the test.

4 Results and Discussion

The variables that affect the surface temperature required to initiate combustion in the steadily flowing fuel-air mixture are the flow velocity, mixture density, inlet-mixture temperature, fuel-air ratio, and the type of fuel. The time available for this study required that the investigation be limited to only a part of the problem. It was therefore decided to restrict the investigation to determination of the effect of flow velocity on surface temperature required for ignition at various free-stream densities. Ethanol was chosen as a fuel because of its availability at constant chemical composition, and for comparison with the work of Barkah and Davis. Stoichiometric fuel-air ratio was maintained because of Davis' report on the difficulty of reproducing results for rich mixtures. Free-stream temperature was held constant at 634°R. This value represents a compromise between ease of heating the mixture and the maximum surface temperature obtainable. The test section temperature required to initiate combustion was determined over a flow velocity range from 20 to 70 feet per second, at free-stream densities of 0.0575, 0.0484, and 0.0393 lbs. per cu. ft. Flashback and burning in the nozzle became troublesome at lower velocities. The limited power output of the induction heater and the safe working temperature of the test section material became a limitation in the high velocity, low density range.

The tabulated data are presented in Table I. The corrections applied to the observed data are discussed in Appendix I. Of particular interest is the correction of the pyrometer reading for the emissivity of the metal observed. Reliable data were found for the emissivity of Nicrome V (Ref. 4) but wide variations were found in the literature for the emissivity of stainless steels, and no specific information was found regarding the 303 stainless steel used in runs 1-6. This prevented a good comparison of the results with steel and Nicrome V test sections.

The temperature versus velocity curves for the Nicrome V test sections are shown in Fig. 6.

Examination of the temperature-velocity curves reveals that the surface temperature required for ignition increases with an increase in velocity, forming a concave downward curve. The curves appear to be asymtotically approaching a limiting temperature for each density; the lower the density, the higher the maximum temperature. Thus at some temperature and density, and increase in velocity will require no increase in temperature to obtain ignition. The velocity range studied is too limited to allow an estimate of this maximum temperature.

Runs 8-14 were made with a 0.130 inch orifice in the air system in an attempt to establish a curve in the low flow velocity regime. However, at velocities below 25 ft. per second, the flame propagated upstream into the nozzle and stabilized on the fine mesh screen that was located there to prevent further flashback. When this burning in the nozzle occurred, the CO_2 extinguishing system had to be operated to keep the nozzle from overheating. When the cold CO_2 came in contact with the hot test section, it caused the test section to warp out of shape and distupt the flow. Therefore, these low velocity runs were discontinued. It would be desirable to obtain data in this region to see if a curve can be established down to zero flow velocity. Smith and Stinson (Ref. 5) list the minimum ignition temperature of ethyl alcohol as 738°F and it would be valuable to discover if the low velocity curves intersect at this point. The data obtained could not be projected to zero velocity with any accuracy.

The concave-downward tendency of the temperature-velocity curves previously mentioned was also noted by Barkah, (Ref. 2). The data is directly comparable only at a density of 0.0575 lbs. per cu. ft. For this case, Barkah's data is about 25°F lower which represents a rather small difference for the two heating methods.

This concave-downward tendency has also been predicted qualitatively from examination of the theoretical equations (Ref. 3).

The temperature, velocity, and reaction profiles depend on the product of a term involving the density and velocity with an exponential term including the surface temperature. Because of the strong effect of the exponential term, it is expected that the curve would be concave downward.

The theory indicates that for a reaction rate following the Arrhenius equation of the second order ignition will occur at the same temperature for the same value of density divided by velocity, if the other variables are held constant. If the theory applies, then the temperature-velocity data at different values of density should be reduced to a single curve when the temperature is plotted versus density-to-velocity ratio. A plot of the data on this basis is shown in Fig. 7, together with Barkah's data for the same free-stream temperature. Also with this theory the velocity at which ignition will occur at the same temperature for a different density may be predicted from a given set of experimental data. Such predicted curves using the 0.0484 lbs. per cu. ft. data as a base are shown in Fig. 6.

It may be seen that the theory comes close to correlating the data on this basis. However, a significant trend is noted which cannot be ascribed to the reproducibility of the data. This is that the points at higher density consistently fall at lower temperatures than the lower density points.

An explanation for this trend has been proposed on the basis of probability. The incipient ignition condition which is to be determined is not a steady-state condition. Assuming small random fluctuations in all the variables as the surface temperature is increased a temperature will be reached at which an occasional ignition will occur. At a higher temperature the frequency of ignition will increase. If the phenomenon is such that the rate of change of frequency of ignition with temperature varies with free-stream density, then there is a possibility of establishing a different ignition criterion at different densities. At a low ignition frequency there is less probability of observing an ignition in a given

observation period than at a higher frequency, and a different temperature would be interpreted as the incipient ignition point. No measurement of ignition frequency has been attempted and a positive answer to this question must await further investigation.

In spite of this trend toward lower temperature at higher density the data is very well correlated by the theory. No point lies more than 20 degrees from a mean curve through the data. It may be concluded, therefore, that within the limits investigated the theoretical prediction that ignition will occur at the same temperature for the same ratio of density to velocity is closely verified by the data.

Some qualitative observations may be of value. It was noted that the temperature of the test section rose very rapidly after ignition occurred. This indicates that the flame is stabilizing at the upstream end of the heated section. The heating of the test section after ignition is more rapid at higher free-stream densities. The flame is quite long, the end not being visible in the two foot sight glass even at low flow velocity. The flame is quite unsteady immediately after ignition, becoming more steady as the test section temperature rises. The flame was generally pale blue, with occasional flashes of yellow.

5 Conclusions and Recommendations

An increase in velocity was found to require an increased surface temperature to initiate combustion. In the higher velocity range, the required increase in surface temperature is less than in the low velocity range for the same change in velocity. The data at different densities are closely correlated by plotting surface temperature versus the ratio of density to velocity. This verifies that the reaction proceeds very nearly according to the Arrhenius equation of the second order. However, a tendency toward ignition at lower temperatures at the same velocity-to-density ratio for the high density data was noted, and should be investigated over a wider density range.

The apparatus used seems well suited to an investigation of this type. It is therefore recommended that the investigation be continued with substantially the same equipment. An effort should be made to obtain a test section material with a higher safe working temperature than Nichrome V. This will permit investigation of a higher velocity and lower density range. A higher powered induction heating generator should be used. This will allow a heating coil with fewer turns to be used, which will allow more flexibility in coil spacing and should result in a uniform temperature distribution over a larger percentage of the test section. Also with more power, higher test section temperatures can be obtained. The effect of density should be investigated over a greater range in order to establish more positively the nature of the trend toward lower ignition temperatures at high density for the same value of density to velocity ratio. The velocity range should be extended to include both lower and higher velocities. The effect of the additional variables remaining in the problem should be investigated.

APPENDIX I

CONTROL AND MEASUREMENT

The reproducibility of any experiment is dependent on the precision with which each of the variables can be controlled and measured. In this investigation these variables are:

1. Air flow
2. Fuel flow
3. Condition of the test section
4. Inlet-mixture temperature
5. Test section temperature
6. Nozzle wall temperature

1. Air flow

The air flow was metered with an ASME square-edged orifice in a two inch pipe. The pressure difference across the orifice was measured with a water manometer, and the pressure ahead of the orifice by a mercury manometer. The air temperature was determined by a mercury thermometer in the pipe ahead of the orifice. Orifices of 0.130 in. and 0.230 in. were employed, depending on the flow rate desired. The larger orifice was suitable for test section velocities of about 28 ft/sec. (depending on the density) up to the maximum velocity investigated. The smaller orifice was used for the lower flow rate range. Orifice calibration curves are shown in Figs. 8 and 9.

An error of ± 0.5 per cent may be introduced into the air flow measurements by the ASME orifice.

The differential pressure across the orifice (ΔP) tended to fluctuate approximately ± 0.05 in. H_2O, and caused an error of about ± 0.2 per cent in the air flow over the range investigated. During a run, an operator was constantly alert for changes in the pressures which would result in an incorrect measurement. If a change occurred just prior to ignition, the run was repeated.

The pressure ahead of the orifice (P_1) and the inlet pressure (P_o) were fairly constant and could be measured to within 0.05 in. Hg.

Since this entire investigation was made with sub-atmospheric pressures in the test section, any leakage at the upstream test section seal would tend to decrease the fuel-air ratio. As may be seen from the plot of pressure versus time (Fig. 5), it required over four minutes for the pressure on the entire system to drop from 10 in. Hg. to 0.5 in. Hg. This is a substantial improvement over Barkah's and Davis' installations.

2. Fuel flow

The fuel flow was metered with a Fischer and Porter rotometer with a 06-150 tube and a 3/32 in. diameter glass ball float. The installation was calibrated for ethanol by means of a balance and electric timer. Fuel was supplied by a gear pump driven by an electric motor. Fuel pressure was maintained constant at 24 psig with a pressure regulator. Fuel temperature was kept constant at 79°F by regulating the water flow through a heat exchanger in the fuel line. The rotometer calibration is shown in Fig. 10.

It is possible to read the rotometer to within one-half of a division on the scale. In the low flow regime this is approximately a two per cent error in the fuel flow. At high flows the error decreases to 0.05 per cent.

The fuel flow was adjusted prior to each run to give a stoichiometric fuel-air ratio. The effect of small variations from the stoichiometric ratio is unknown.

3. Condition of the test section

With the apparatus used for this investigation, the factor which most affects the reproducibility is the condition of the test section. As long as the flow is not disrupted by the test section warping out of round, the data may be reproduced to within 10°F. When the flow is disrupted, the temperature distribution also is disrupted, and data taken cannot be correlated.

4. Inlet-mixture temperature

The inlet-mixture temperature was measured by a shielded thermocouple upstream of the nozzle entrance. The shielding was provided to reduce errors due to radiation from the test section. The temperature was controlled by adjusting the steam flow to the jacket on the inlet mixing tank and to the steam coil around the piping between the mixing tank and the nozzle.

An electric heater ahead of the mixing tank was also available, but preliminary tests indicated that its use did not substantially increase the mixture temperature.

A copper-constantan thermocouple was used to measure the inlet-mixture temperature. The cold junction was maintained at room temperature and compensated for by adjusting the potentiometer. The potentiometer used was manufactured by Leeds and Northrup and could be read to within 0.05 millivolts. This corresponds to an error of $\pm 2°F$ throughout the range of temperatures measured.

5. Test section temperature

The temperature of the test section was measured with an optical pyrometer. The temperature was controlled by adjusting the power input to an electrical induction coil. The temperature distribution could be varied by adjusting the coil spacing.

The test section temperature could be adjusted to any temperature up to approximately 2200°F. Under normal operating conditions the temperature would remain constant once it was set. However, surges in the power output of the radio-frequency generator would occur when other electrical equipment in the laboratory caused a change in the voltage input to the generator. This resulted in a momentary fluctuation in the test section temperature and the run was delayed until the transient in the power source disappeared.

The ability to increase the test section temperature in small increments plays an important part in the accuracy obtained. The test section temperature could be advanced in increments as low as 3°F. Even closer precision was added to the operation since the output of the radio-frequency generator could be controlled while

following the increase in test section temperature with the optical pyrometer. This tended to eliminate any error which may have been introduced by the heating process or by the rate of heating.

The optical pyrometer used to measure the test section temperature was of the disappearing filament type and was manufactured by Leeds and Northrup. The temperature scale was calibrated in ten degree increments. It was found that observations could be reproduced by different experienced operators to within three degrees. The instrument error was checked by comparison with a standard optical pyrometer maintained by the Heat Measurement Laboratory of the Massachusetts Institute of Technology. The variation of the instrument from the standard was found to be within the reproducibility of readings throughout the temperature range at which measurements were made.

An optical pyrometer is so calibrated that it will measure accurately the temperature of a theoretical "black body." The radiation emitted by any actual material is less than that of a black body, and therefore the temperature measured with a pyrometer will be less than the true temperature. If the emissivity of the material is known, the pyrometer reading may be corrected to true temperature by use of Wien's law, which states

$$1/T - 1/T_{apparent} = \ln \mathcal{E} / \text{constant}$$

where $\mathcal{E}$ is the emissivity. Roesser (Ref. 4) found that the emissivity of an 80 per cent nickel and 20 percent chromium alloy varied over the range of temperatures of interest from 0.88 to 0.92. Ref. 4 contains a tabulation of apparent and true temperatures which has been plotted in Fig. 11 and used for determining the true temperature.

The initial series of tests was made with 303 stainless steel. The literature (e.g. Ref. 6) reveals a wide range of emissivity for various stainless steels under different conditions. Since no specific information was found regarding 303 stainless steel, no attempt has been made to correct the observed temperature of these tests. It is noted that a reasonable value of emissivity could be chosen which

would correlate the stainless steel data perfectly with the Nicrome V data.

6. Nozzle wall temperature

The flow of coolant in a circumferential cooling passage around the nozzle was regulated to maintain the nozzle wall temperature between 100°F and 120°F. A coolant flow was set up and the temperature taken when the system reached equilibrium. Since it was believed that minor changes ($\pm$10°F) in the nozzle wall temperature did not affect the accuracy of the test, no attempt at more precise control was made. A copper-constantan thermocouple embedded in the nozzle wall and connected to a Leeds and Northrup potentiometer was used to measure the nozzle wall temperature.

APPENDIX II

TEMPERATURE DISTRIBUTION

The temperature distribution desired along the test section would have an infinite slope at the upstream and downstream ends with a zero gradient between. Although it is impossible to obtain this theoretical distribution, a reasonable approximation to the desired distribution is shown in Fig. 4. The temperature recorded in the data ($T_{w\ apparent}$) was taken in the middle of the flat portion of this curve. As is also shown in Fig. 4, a coil with constant pitch gives a parabolic curve for the variation of temperature along the test section.

The theory of induction heating states that the thermal power generated in the material varies with the inductance of the coil. The inductance of a coil varies with the pitch of the coil. From these facts, it was deduced that the temperature along the test section could be controlled by varying the pitch of the coil: a constant pitch in the center of the test section for constant heat input with an increase in pitch at the ends where the conduction losses are high. The proper coil spacing was obtained by a trial-and-error method. The spacing shown in Fig. 4 is considered to be the optimum that can be obtained with a 1-kilowatt induction heater.

Trial and error methods were also used to determine the correct number of turns for the coil. Coils of 3/4 inch inside diameter having 12, 16, and 19 turns were made from 1/8 inch copper tubing. To get a greater number of turns per inch the tubing was flattened by compressing the coils in an arbor press. The coils were then stretched to obtain the desired spacing. The pitch of the coil with 12 turns was so great that the test section was cold between each turn. The coil with 19 turns had to be compressed so much to make it two inches long (including spacing between each coil) that the rate of coolant flow through the tubing was not sufficient for steady operation. Therefore, the 16 turn coil was used.

It was felt that the symmetry of the test setup would insure a constant circumferial temperature at each cross-section. This proved to be true if care were taken in aligning the test section with the nozzle. Upon being heated and cooled a few times, the test section warped, disrupted the flow and caused uneven temperatures around the periphery. To increase the life of each test section, a flange was placed at each end of the test section (Fig. 2). Using CO_2 at 60 psi to extinguish the flame also tended to warp the test section, therefore the pressure on the CO_2 system was reduced to 20 psi and then used sparingly.

In a preliminary test the pyrometer was used to measure the inside temperature of the heated test section by taking an angling observation from the top. When this reading was compared with the temperature taken on the outside of the test section at approximately the same spot, no measurable difference was obtained. The accuracy of this method is doubtful. However, heat transfer calculations as shown in Appendix IV show only an 8°F difference between the outer and inner surfaces in the worst situation. Therefore, the temperature of the test section was measured on the outer surface by means of an optical pyrometer.

APPENDIX III

INDUCTION HEATING

Induction heating is the heating of a conducting material, either magnetic or non-magnetic, by means of its own I^2R losses due to currents induced in the material when it is placed in a varying magnetic field. The material is placed either within or near a coil carrying current at a frequency from 200 to 450 kilocycles a second. When the coil is connected to a radio-frequency generator, a large amount of radio-frequency current flows. This primary current induced electromotive forces in the material to be heated, and secondary load current (induced current) flows in the material as a result. Since all materials have some electrical resistance, the induced current produces heat in the material.

The R-F generator used in this investigation was a Westinghouse 1-kilowatt machine designed especially for colleges and laboratories for experimental work and demonstrations. The equipment was not designed for continuous operation at maximum output. For normal operation, its output should be limited to between 800 and 900 watts. During this study, maximum output was required only at high velocities or low densities, and then only for short periods of time.

The Westinghouse 1-kilowatt radio-frequency generator is enclosed in an aluminum cabinet and is mounted on castors to allow it to be moved around by one person. The controls are mounted on a sloping section of the front panel. The power supply is a conventional full-wave, filtered rectifier circuit. Protection for the various circuits is provided by an overload relay that removes high voltage from all tubes when the equipment is operated above its maximum rating. The generator draws approximately 1.8 kilowatts at 115 volts and 60 cycles when operated at its rated output.

When the safety precautions and operating instructions given in the instruction book provided with the equipment are followed, a safe and rapid method of heating the test section is the result. A two-to-one pulley arrangement on the plate voltage control knob made it possible to vary the test section temperature in three degree increments. Fig. 1 schematically illustrates the secondary circuit.

APPENDIX IV

SAMPLE CALCULATIONS

A. Establishing desired operating conditions:

Desired conditions: $\rho_o = 0.0575$ lbs/cu. ft.

$V = 30$ ft/sec

$T_o = 634°R$

Free stream pressure

$$p_o = \rho_o R T_o \left(\frac{29.92}{2116}\right)$$

$$= (0.0575)(51.4)(634)\left(\frac{29.92}{2116}\right)$$

$$= 26.5 \text{ in. Hg. abs.}$$

Mass flow

$$w = \rho V A$$

$$= 0.0575\ (30)\ \left(\frac{\pi}{4}\right)\ \left(\frac{1}{2}\right)^2\ \left(\frac{1}{12}\right)^2$$

$$= 0.00234 \text{ lbs/sec}$$

Air flow

$$w = w_f + w_a$$

$$w_f/w_a = 0.111 \text{ (stoichiometric)}$$

$$w = 1.111\ w_a$$

$$w_a = \frac{w}{1.111} = 0.00211 \text{ lbs/sec}$$

Enter orifice calibration curve with this value and select approximate value of ΔP. Adjust valves to obtain desired P_o and approximate ΔP. Read P_1 and T_1 and apply correction to obtain more nearly correct air flow:

$$w_a = w_{curve} \sqrt{\frac{P_1}{29.9} \times \frac{520}{T_1}}$$

Read new ΔP. Readjust valves to obtain new ΔP and check P_1. If there is any change, repeat procedure. Usually, one iteration is sufficient.

Fuel flow

$$w_f = 0.111\ w_a$$

$$= 0.000234 \text{ lbs/sec}$$

Obtain proper rotometer reading from rotometer calibration curve. (Air flow may have to be readjusted after adding fuel.)

B. Temperature Gradient Through Test Section Wall

The temperature difference between the inner and outer wall of the test section may be estimated by a simple calculation. The maximum energy input to the system is one kilowatt from the induction heater. Most of the heat loss is by radiation from the outside. As a limiting condition it is assumed that half the heat is transferred to the fluid on the inside of the tube and that the induction heating only penetrates 0.005 in.

$q = 0.5$ kw

$x = .010$ in $= 0.0254$ cm

$k = 0.136$ watts per sec per cm per °C

$A = \pi(1/2)2 \times 2.54^2 = 20.3$ cm^2

$$\frac{q}{A'} = k\frac{\Delta T}{\Delta x}$$

$$\Delta T = \frac{q\,\Delta x}{k\,A'}$$

$$= \frac{500\ (0.0254)}{0.136\ (20.3)}$$

$$= 4.6°C$$

$$= 8.3°F$$

Actually less than one kilowatt of energy is transferred to the work, and of this considerably less than one-half is transferred to the fluid inside the tube, due to the large radiation loss externally, and end losses. Also the penetration of the induction heating is probably somewhat greater. All of these factors tend to make the temperature difference between inner and outer wall smaller.

BIBLIOGRAPHY

1. Davis, J.W., "Design of a Steady-Flow Apparatus for Studying Surface Ignition", M.S. Thesis, Department of Mechanical Engineering, M.I.T., 1955.

2. Barkah, K., "Surface Ignition in a Steady-Flow Apparatus", M.S. Thesis, Department of Mechanical Engineering, M.I.T., 1956.

3. Toong, T.Y., "Ignition and Combustion in a Laminar Boundary Layer Over a Hot Surface", Paper submitted for presentation at the Sixth International Symposium on Combustion, Yale University, August 19 through 24, 1956.

4. Roesser, W.F., "Spectral Emissivity (At 0.65μ) of Some Alloys for Electrical Heating Elements", Proc. A.S.T.M., Vol. 39, 1939.

5. Smith, M.L. and Stinson, C.W., "Fuels and Combustion", McGraw-Hill, New York, 1952.

6. McAdams, W.H., "Heat Transmission", McGraw-Hill, Third Edition, 1954.

TABLE I - TABULATED DATA

Run	Date	Bar Press InHg	p_1 InHg Gage	T_1 °R	Δp InH_2O	p_o InHg Gage	T_{noz} °F	Roto Read	T_w App °F	T_o °R	p_o InHg	.3	$w_a x 10^3$ lb/sec	$w_f x 10^4$ lb/sec	w_f/w_a	V ft/sec	T_w °R	Remarks
1	4/6	29.9	-2.5	539	6.2	-3.4		8.80	2021	634	26.5		2.08	2.34	.112	29.6		See Note 2
2	4/10	29.9	-2.2	540	6.2	"		"	2044	"	"		"	"	"	"		
3	4/11	30.0	-2.0	"	11.5	"		10.10	2055	632	26.6		2.83	3.10	.109	39.8		
4	"		-1.7	"	17.4	"		11.85	2085	634	"		3.47	4.15	.120	50.8		
5	"		-1.1	"	25.4	-3.5		12.70	2111	"	"		4.22	4.65	.110	59.6		
6	"		-2.6	"	6.2	-3.4		8.80	2020	"	"		2.08	2.34	.112	29.5		
7	4/19	29.8	-0.8	"	31.6	"		8.15	2016	"	26.4		1.75	1.95	.111	25.0	2493	See Notes 1 and 2
8	4/21	29.9	-1.7	539	19.6	"	120	7.30	2006	"	26.5		1.40	1.56	"	19.9	2483	See Note 2
9	"		-0.8	"	31.6	"		8.15	2024	"	"		1.76	1.95	"	24.9	2501	
10	"		-10.0	"	20.6	-11.8		6.70	2081	"	18.1		1.20	1.34	.112	24.9	2560	
11	"		-9.2	"	30.3	"		7.42	2111	633	"		1.45	1.60	.110	30.1	2590	
12	"		-8.9	"	35.4	"		7.72	2124	"	"		1.62	1.74	"	33.6	2603	
13	"		-1.7	"	31.6	-3.4		8.15	2018	"	26.5		1.73	1.95	.113	24.6	2495	Burning in nozzle
14	"		-10.8	"	10.6	-11.8		5.91	2051	"	18.1		0.91	1.07	.118	19.0	2529	Burning in nozzle, Not plotted, w_f/w_a high
15	"		-2.4	"	8.8	-3.4		9.43	2051	637	26.5		2.47	2.70	.109	35.1	2529	
16	"		"	"	"	"		"	2052	633	"		"	"	"	34.9	2530	
17	"		-2.0	"	14.6	"		10.80	2092	634	"		3.17	3.52	.111	45.0	2571	
18	"		"	"	14.5	"		"	2088	"	"		3.16	"	"	44.9	2567	
19	"		-1.4	"	21.8	"		12.15	2109	"	"		3.90	4.32	"	55.4	2588	
20	"		-0.8	"	29.6	"		13.38	2080	"	"		4.58	5.05	.110	65.0	2559	No ignition
21	"		-11.2	"	4.4	-11.8		7.42	2104	"	18.1		1.45	1.60	"	30.1	2583	
22	"		-11.1	"	6.0	"		8.00	2130	"	"		1.70	1.87	"	35.3	2610	
23	"		-10.9	"	7.8	"		8.50	2162	626	"		1.93	2.16	.112	39.6	2642	Not plotted, p_o high
24	4/24	30.2	"	538	"	"	115	"	2141	634	18.4		1.99	2.15	.108	38.8	2621	Not plotted, p_o high, w_f/w_a low
25	"		-11.2	539	7.8	-12.1		"	2151	"	18.1		1.93	"	.111	40.1	2631	
26	"		-11.0	"	12.2	"		9.38	2189	"	"		2.41	2.67	"	50.1	2670	
27	"		"	"	9.8	"		8.91	2172	"	"		2.18	2.40	.110	45.3	2652	
28	"		-1.0	"	29.4	-3.7		13.38	2134	"	26.5		4.56	5.05	.111	64.7	2614	
29	"		-1.0	"	29.5	"		"	2135	"	"		"	"	"	"	2615	
30	"		-0.7	"	34.5	"		14.00	2152	637	"		4.91	5.45	"	70.0	2632	
31	"		-0.7	"	34.5	"		"	2148	634	"		4.91	"	"	69.7	2628	
32	"		-1.4	540	25.6	"		12.72	2128	"	"		4.23	4.65	.110	60.0	2608	
33	"		-1.4	"	25.7	"		"	2125	"	"		"	4.67	"	"	2615	
34	"		-2.0	"	17.8	"		11.85	2101	"	"		3.50	4.15	.119	50.0	2580	Not plotted, w_f/w_a high
35	"		-2.5	"	11.4	"		10.12	2071	633	"		2.81	3.11	.111	39.8	2551	

TABLE I - TAP

Roto Read	T_w App °F
8.80	2021
"	2044
0.10	2055
1.85	2085
2.70	2111
8.80	2020
8.15	2016
7.30	2006
8.15	2024
6.70	2081
7.42	2111
7.72	2124
8.15	2018
5.91	2051
9.43	2051
"	2052
10.80	2092
"	2088
12.15	2109
13.38	2080
7.42	2104
8.00	2130
8.50	2162
"	2141
"	2151
9.38	2189
8.91	2172
13.38	2134
"	2135
14.00	2152
"	2148
12.72	2128
"	2125
11.85	2101
10.12	2071

TABLE I (Continued)

Run	Date	Bar Press InHg	p_1 InHg Gage	T_1 °R	ΔP InH_2O	Po InHg Gage	Tnoz °F	Roto Read	T_w App °F	T_o °R	Po InHg		$w_a x10^3$ lb/sec	$w_f x10^4$ lb/sec	w_f/w_a	V ft/sec	T_w °R	Remarks
36	"		-2.9	"	6.4	"		8.80	2024	634	"	.	2.12	2.34	.110	30.1	2501	Burning in nozzle
37	"		-2.9	"	6.5	"		"	2031	635	"	.	"	"	"	30.1	2509	
38	"		-3.1	"	4.5	"		8.15	2015	634	"	.	1.78	1.95	"	25.2	2492	Burning in nozzle
39	"		"	"	"	"		"	"	"	"		"	"	"	"	"		Burning in nozzle
40	4/26	30.2	-7.3	538	5.4	-8.0		8.20	2084	637	22.2	.	1.78	1.98	.111	30.2	2563	
41	"		-7.4	539	4.8	"		7.51	2074	634	"	.	1.67	1.65	.099	27.9	2552	Not plotted, w_f/w_a low
42	"		"	"	4.8	"		7.51	2072	"	"		"	1.63	.098	27.8	2550	Not plotted w_f/w_a low
43	"		-2.9	"	4.4	-3.7		8.80	2040	636	26.5	.	1.74	2.34	.134	25.3	2518	Not plotted, w_f/w_a high
44	"		"	"	"	"		"	2037	"	"		"	"	"	"	2515	" " " " "
45	"		-7.2	"	6.4	-8.0		8.75	2099	633	22.2	.	1.94	2.30	.119	32.9	2578	" " " " "
46	"		"	"	7.4	"	114	"	2095	634	"	.	2.08	2.30	.111	35.1	2574	
47	"		-7.0	"	9.8	"		9.30	2118	"	"		2.38	2.63	"	40.1	2597	
48	"		-6.8	540	12.4	"	117	9.94	2135	"	"		2.67	3.00	.112	45.1	2615	
49	"		-6.6	"	14.9	"		10.46	2148	633	"	.	2.95	3.30	"	49.7	2628	
50	"		-6.3	"	18.4	"		10.95	2157	634	"	.	3.28	3.61	.110	55.3	2637	
51	"		-6.0	"	21.4	"		11.52	2178	633	"	.	3.56	3.96	.111	60.0	2659	
52	5/3	29.9	-2.0	539	14.5	-3.4	112	10.80	2096	"	26.5	.	3.16	3.51	"	44.8	2575	See Note 2
53	"		"	"	"	"		"	2096	634	"	.	"	3.51	"	44.9	"	
54	"		-1.7	"	17.8	"		11.85	2110	637	"		3.50	4.15	.118	50.0	2589	Not plotted, w_f/w_a high
55	"		"	"	"	"		"	2111	634	"		"	4.15	"	"	2590	Not plotted, " " "
56	"		-1.4	540	21.9	"		12.15	2129	634	"		3.89	4.33	.111	55.3	2609	
57	"		-1.1	"	25.6	"		12.72	2140	"	"		4.22	4.67	"	59.9	2620	
58	"		-0.8	"	29.6	"		13.40	2155	"	"		4.56	5.07	"	64.8	2635	
59	"		-0.4	"	34.6	"	108	14.00	2167	"	"		4.91	5.45	"	69.7	2647	
60	"		-6.4	"	12.3	-7.7		9.94	2132	"	22.2	.	2.66	3.00	.113	45.1	2612	
61	"		-6.2	"	15.1	"		10.46	2145	"	"		2.97	3.32	.112	50.3	2625	
62	"		-5.9	"	18.2	"		10.95	2159	"	"		3.26	3.62	.111	55.2	2639	
63	"		-5.7	"	21.3	"		11.52	2179	"	"		3.55	3.97	.112	60.2	2660	
64	"		-5.4	"	25.1	"		12.05	2191	633	"		3.85	4.27	.111	65.2	2672	
65	"		-5.1	"	28.6	"		12.61	2201	"	"		4.13	4.60	"	70.0	2682	
66	"		-10.4	"	14.6	-11.8		9.82	2207	634	18.1	.	2.65	2.94	"	55.0	2688	

Notes

1. 0.130" orifice used for runs 7-13. 0.230" orifice used for all other run
2. 303 Stainless steel test section used for runs 1-6. Emissivity correctio termined.
   First Nichrome V test section used for run 7. Second Nichrome V test sec used for runs 8-51.
   Third Nichrome V test section used for runs 52-66.

BLE I (Cont:

T_w App °F	T
2024	6
2031	6
2015	6
"	
2084	6
2074	6
2072	
2040	6
2037	
2099	6
2095	6
2118	'
2135	'
2148	6
2157	6
2178	6
2096	'
2096	6
2110	6
2111	6
2129	6
2140	'
2155	"
2167	"
2132	"
2145	"
2159	"
2179	"
2191	6
2201	"
2207	6

e used for a

6. Emissivi
cond Nichrom
'.

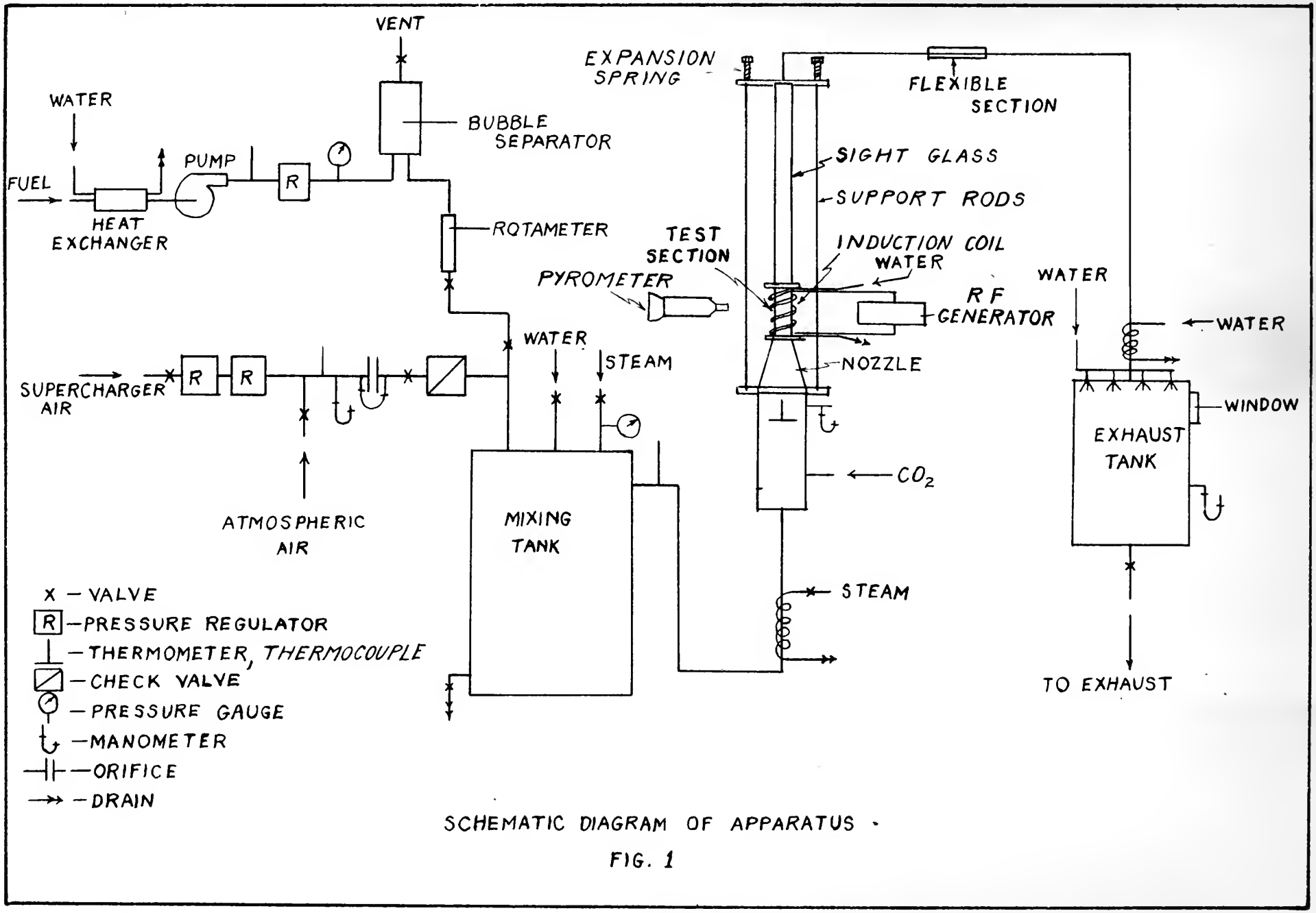

SCHEMATIC DIAGRAM OF APPARATUS

FIG. 1

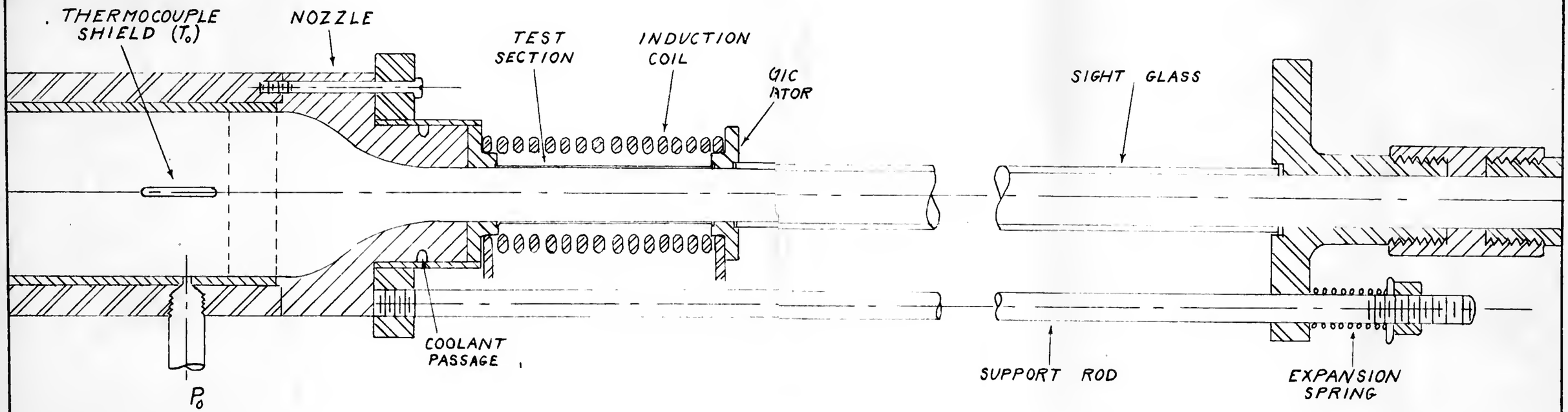

MASS. INSTITUTE OF TECHNOLOGY		
ASSEMBLY		
SCALE 1:1	1956	EWS

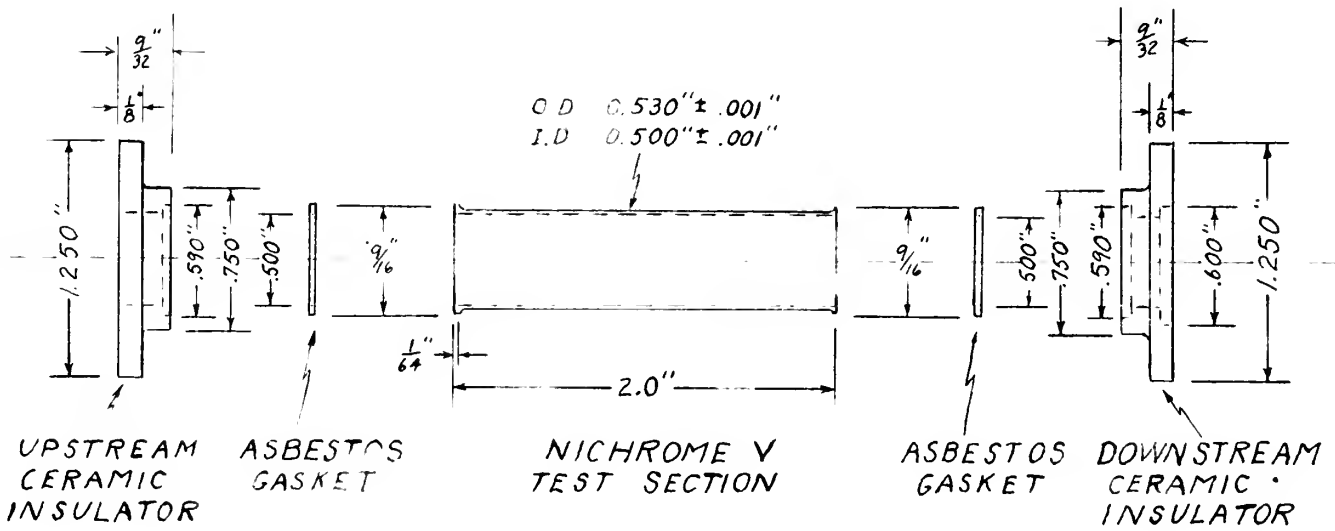

MASS. INSTITUTE OF TECHNOLOGY
TEST SECTION AND INSULATORS
SCALE 1:1 1956 EWS

FIG. 3

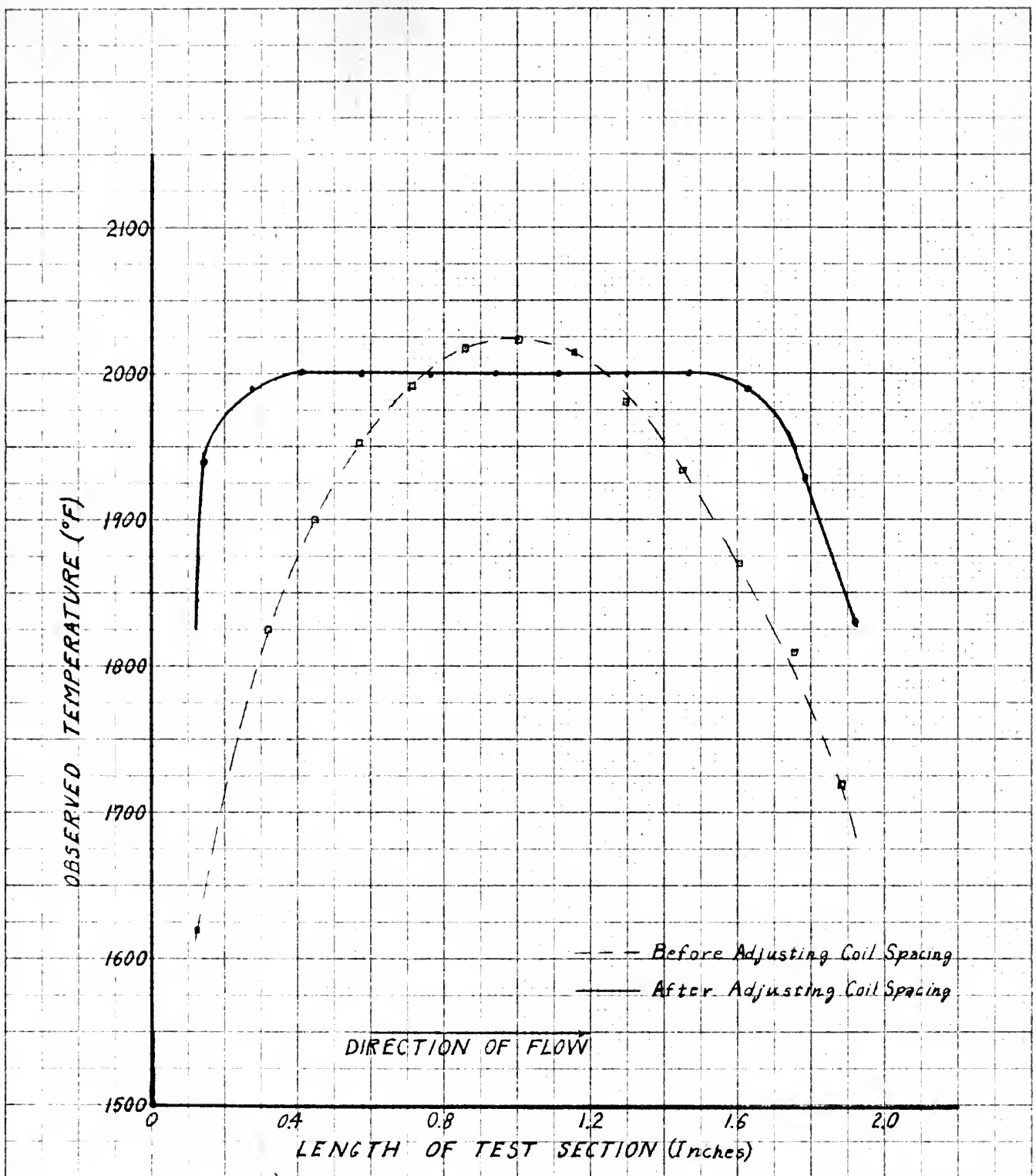

SURFACE TEMPERATURE DISTRIBUTION

FIG. 4

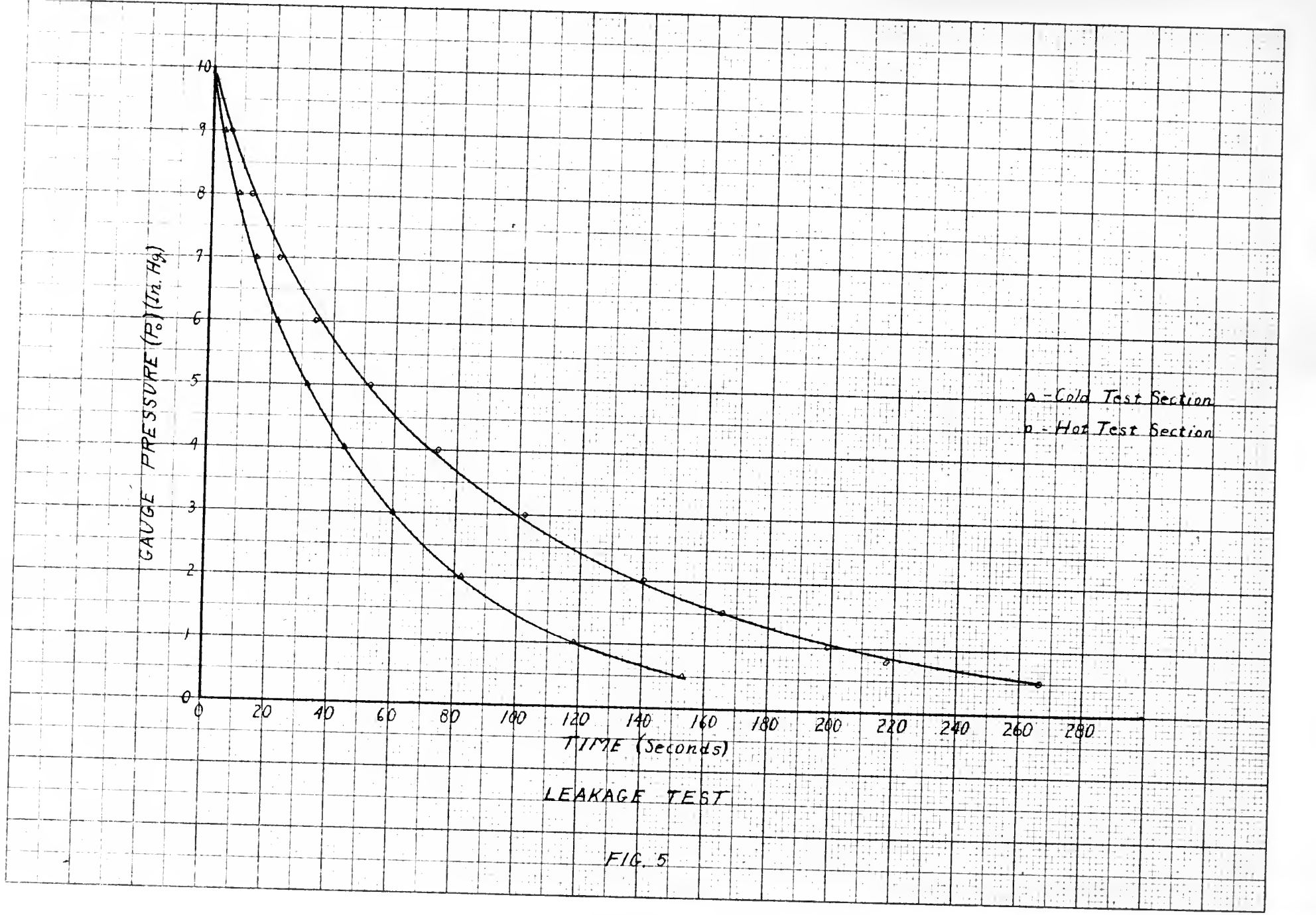

LEAKAGE TEST

FIG. 5

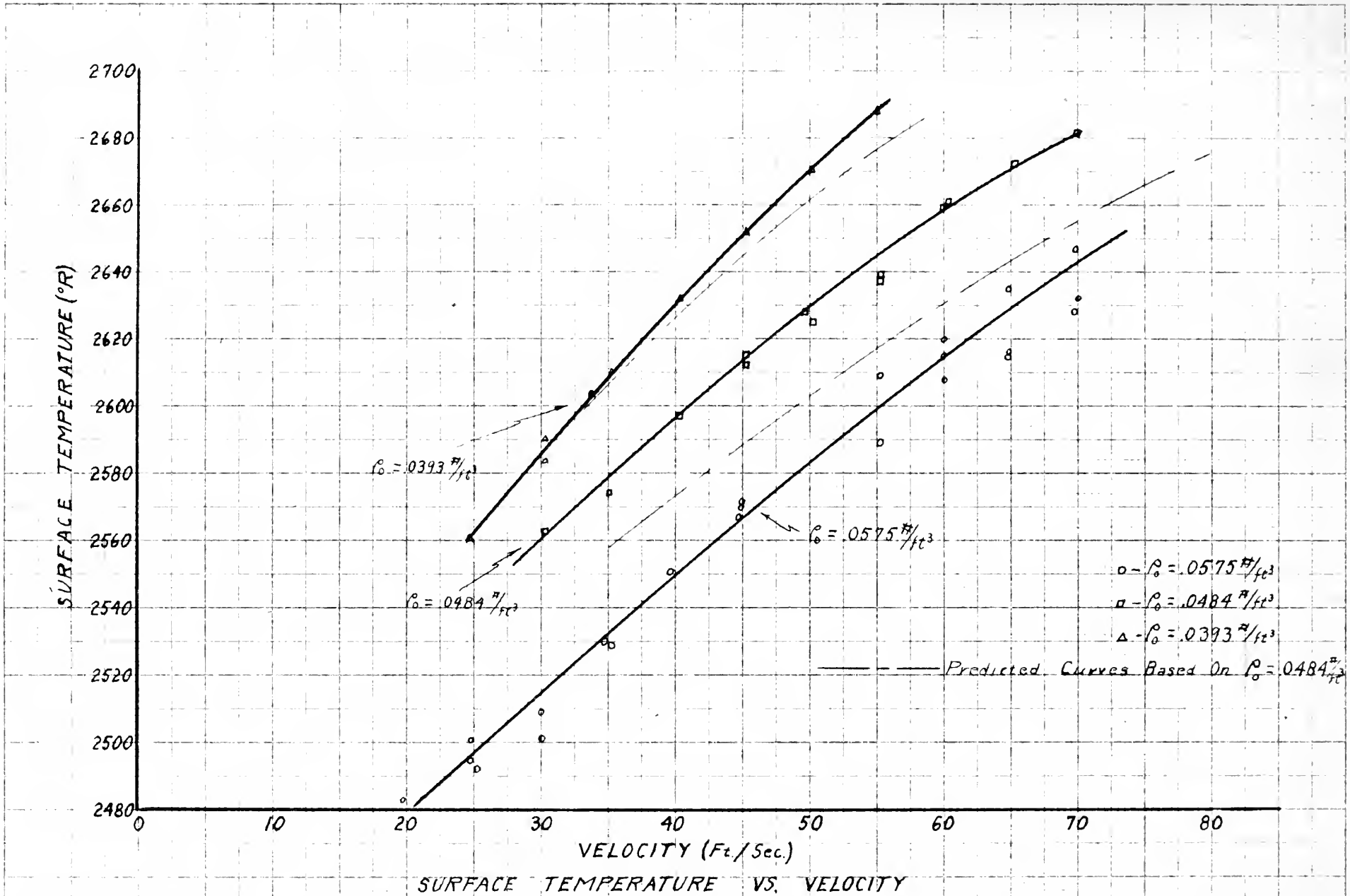

SURFACE TEMPERATURE VS. VELOCITY

FIG. 6

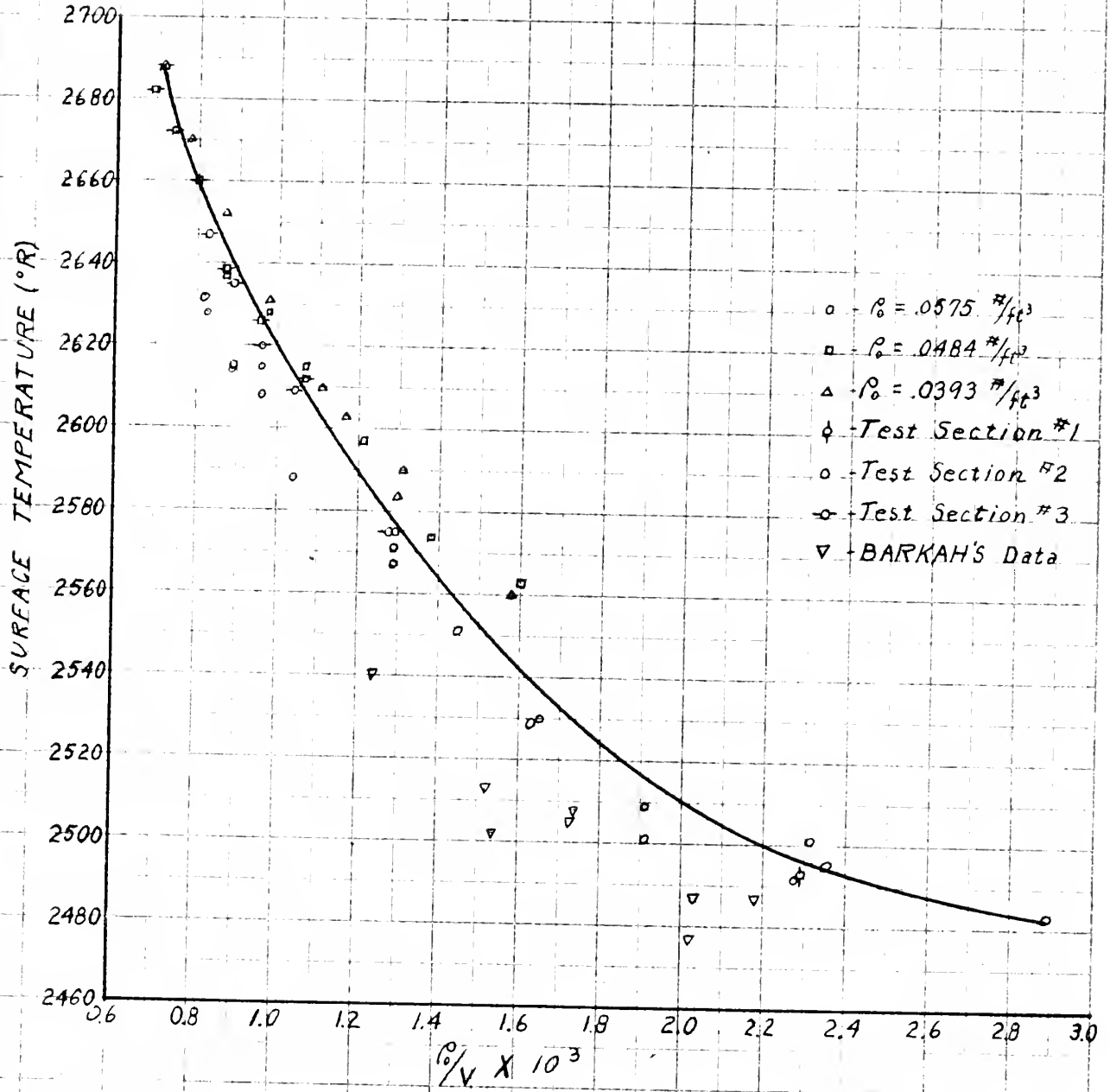

SURFACE TEMPERATURE

V.S.

RATIO OF DENSITY TO VELOCITY

FIG. 7

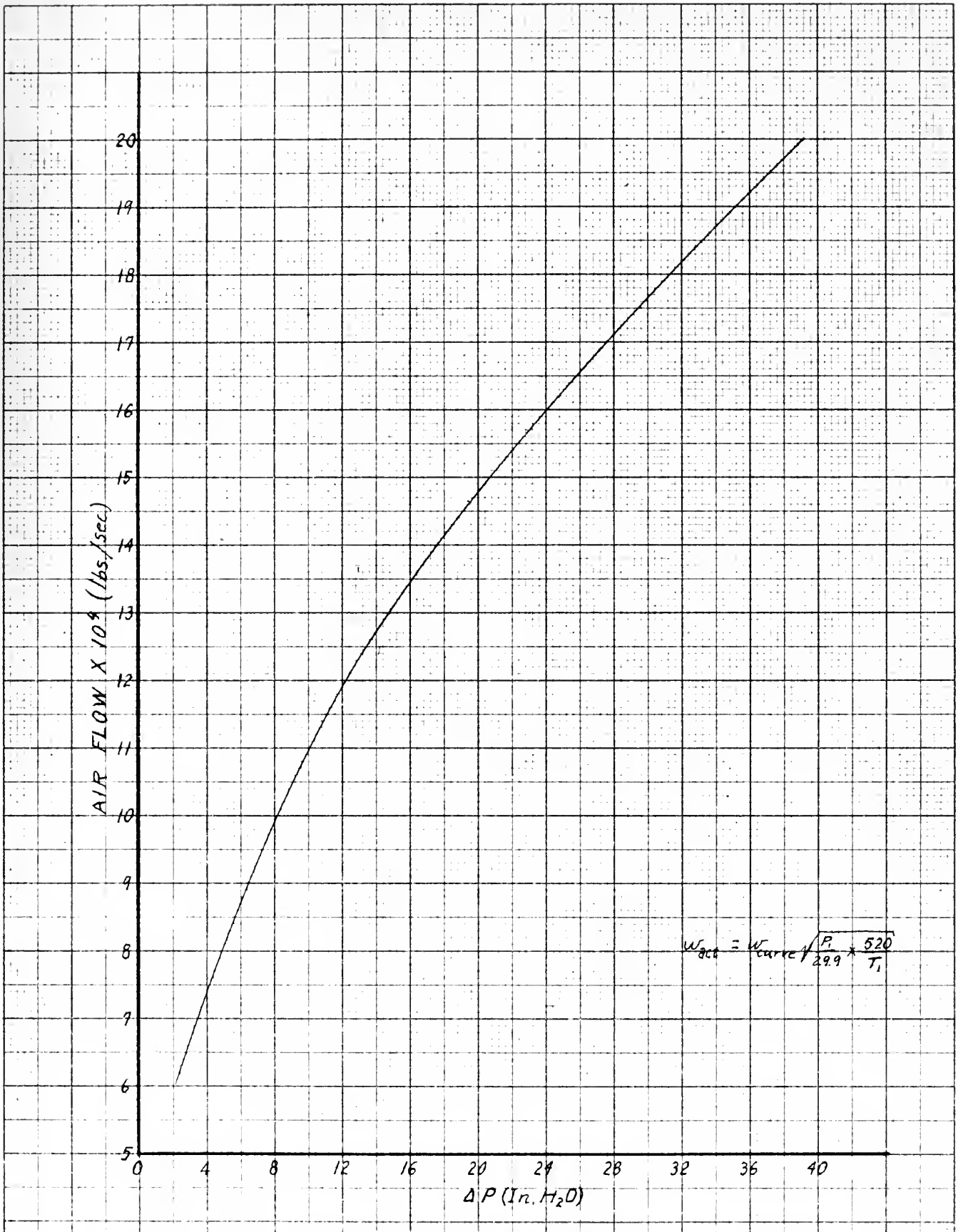

0.130" ORIFICE CALIBRATION

FIG. 8

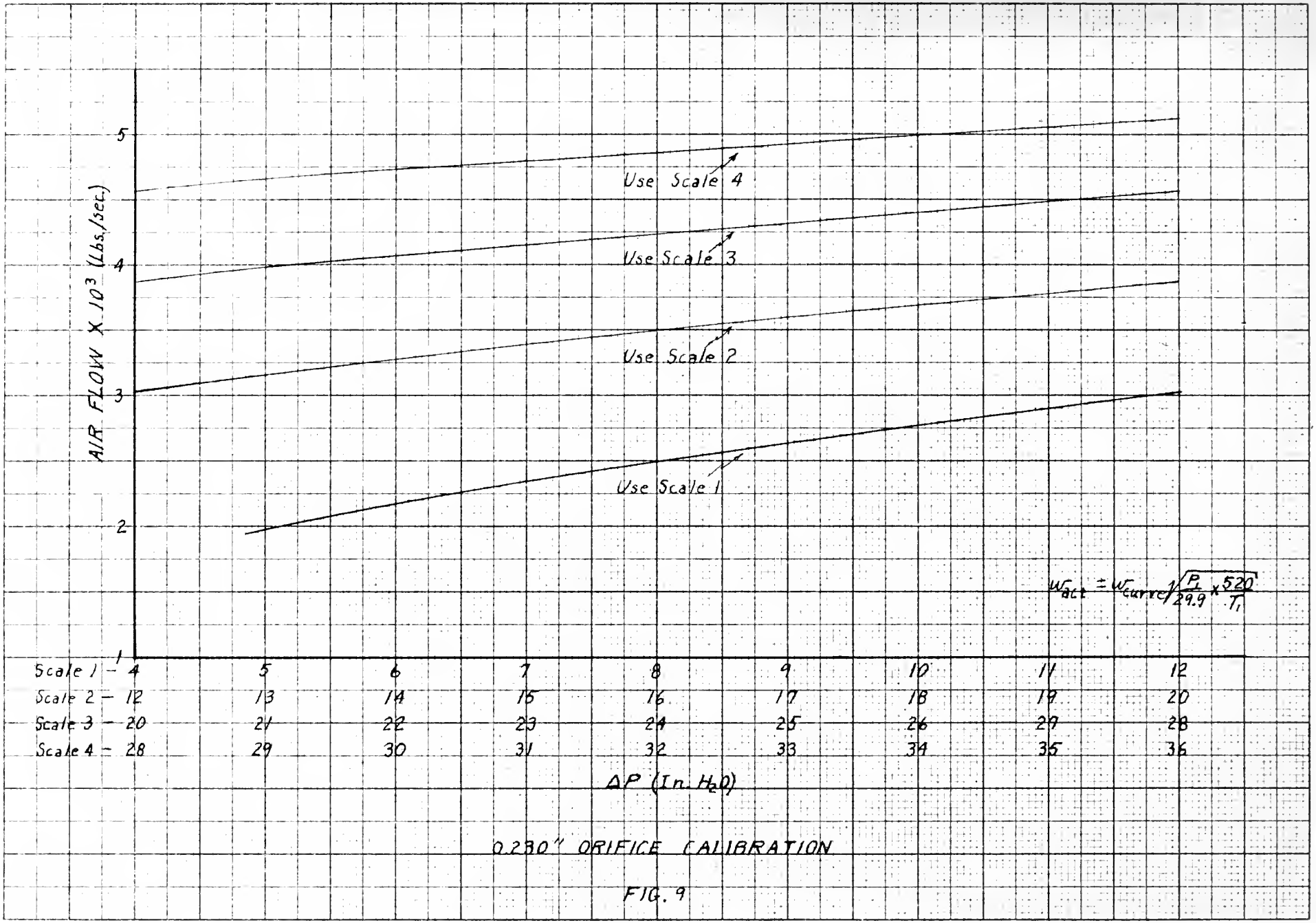

0.230" ORIFICE CALIBRATION

FIG. 9

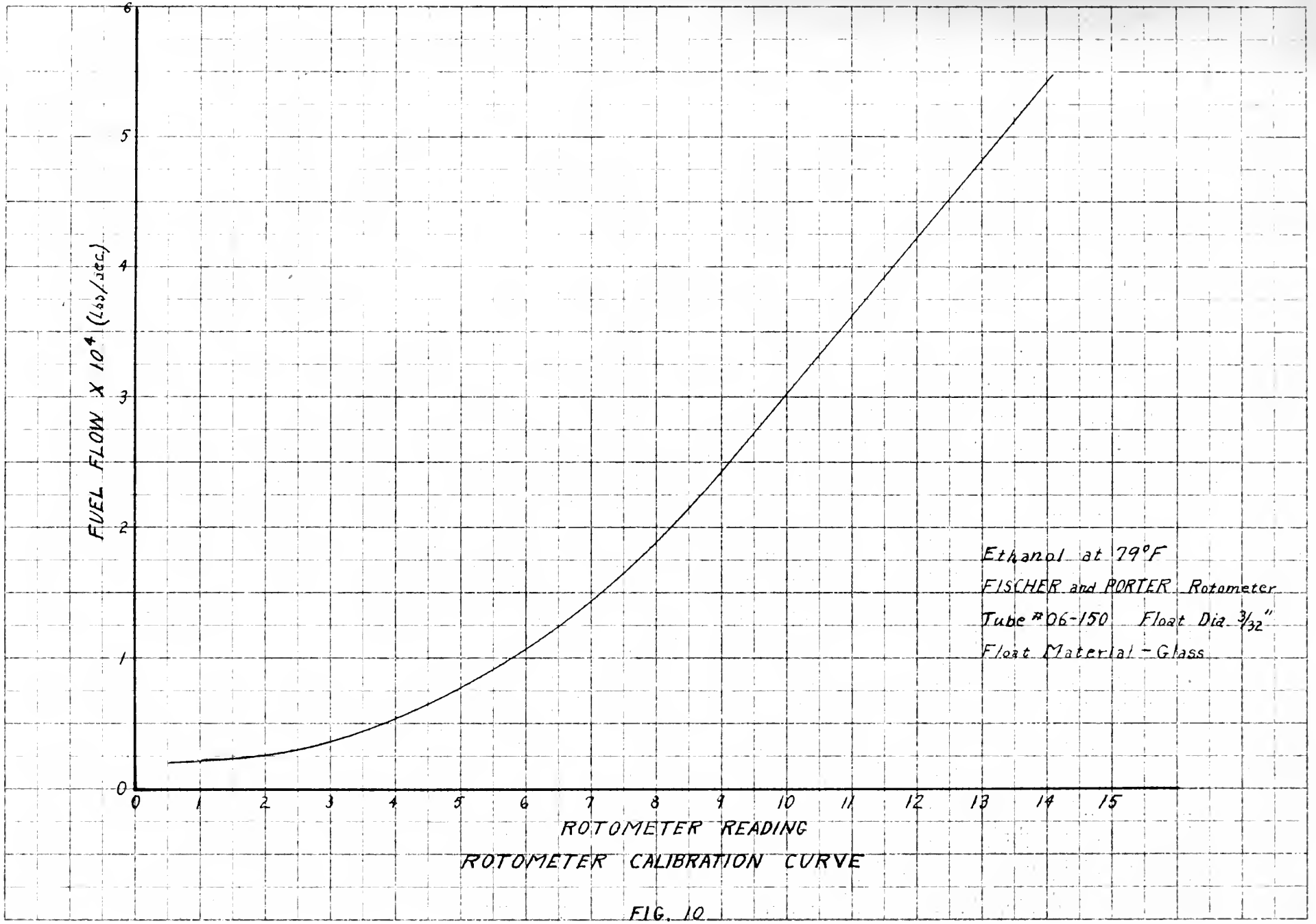

ROTOMETER CALIBRATION CURVE

FIG. 10

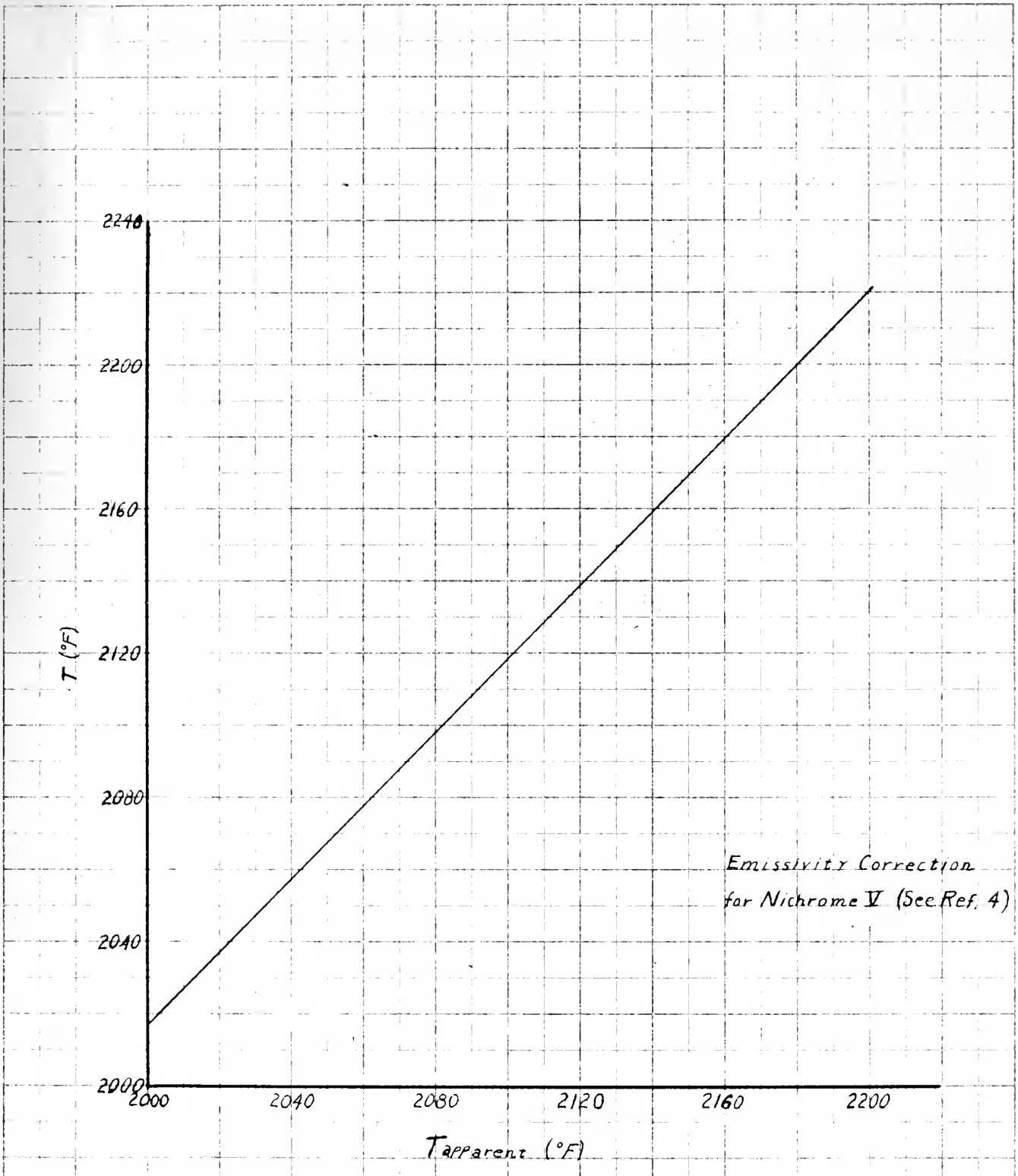

TRUE TEMPERATURE VS. APPARENT TEMPERATURE

FIG. 11